Refractive index changes in amorphous SiO_2 (silica) by swift ion irradiation

O. Peña-Rodríguez J. Manzano-Santamaría J. Olivares A. Rivera F. Agulló-López

A B S T R A C T

The refractive index changes induced by swift ion-beam irradiation in silica have been measured either by spectroscopic ellipsometry or through the effective indices of the optical modes propagating through the irradiated structure. The optical response has been analyzed by considering an effective homogeneous medium to simulate the nanostructured irradiated system consisting of cylindrical tracks, associated to the ion impacts, embedded into a virgin material. The role of both, irradiation fluence and stopping power, has been investigated. Above a certain electronic stopping power threshold (~2.5 keV/nm), every ion impact creates an axial region around the trajectory with a fixed refractive index (around $n = 1.475$) corresponding to a certain structural phase that is independent of stopping power. The results have been compared with previous data measured by means of infrared spectroscopy and small-angle X-ray scattering; possible mechanisms and theoretical models are discussed.

1. Introduction

Silicon dioxide (SiO_2) is a material very abundant in nature that can be considered as a reference dielectric material. Its amorphous phase (silica) has been extensively studied and offers the appropriate network structure to understand the behavior of glasses and ceramics. The properties of silica: transparency, low dielectric losses and chemical inertness, make it the most adequate material for several key technologies going from microelectronics to photonics, e.g. fiber and integrated optics [1]. Moreover, the study of defects created by irradiation in this material is of much relevance for nuclear (both fusion and fission) installations [2] and space applications [3,4].

For ion-beam irradiation one has to consider two basic regimes, one associated to elastic collisional processes and the other one being dominated by the energy deposited by electronic excitation [5]. The first regime is quite universal and the processes are reasonably well understood so that efficient simulation codes are available [6]. The electronic regime, which is particularly dominant for medium – or high – mass ions at high energies, has been less investigated and is less understood, although several theoretical models have been proposed [7–10]. For silica, the damage caused by ion-beam irradiation in the electronic excitation regime is rather scarce [11–18]. In fact, the structure of the damage and the active microscopic mechanisms are not yet fully understood. What it is well ascertained is that point defects, color centers and heavy structural disorder are produced during this process [19] and the atomic network undergoes significant compaction [11–15] due to changes in the distribution of ring sizes [20,21] produced by both, ionization events and atomic collisions. The densification process, which results in an increase of the refractive index, has been found to saturate with fluence [11]. This effect has been investigated by infrared spectroscopy [22,23], and more recently through the associated refractive index changes that allow for light propagation at the irradiated surface (waveguiding) [24].

The purpose of this work has been to improve our experimental information on the irradiation-induced changes of refractive indices by comparing the results of two optical techniques: spectroscopic ellipsometry and dark-mode propagation. The advantages and disadvantages of each technique will be discussed and related to the other methods used for investigation. In particular, the new results provide a better understanding of the compaction kinetics and give some clues on the cumulative character of the electronic damage.

2. Experimental

Two kinds of samples were used in the experiments: pure silica plates (OH content below 5 ppm) of around 7×8 mm^2, purchased from EMS and SiO_2 thin films obtained by thermal oxidation of a silicon substrate (provided by Siegert Consulting e.K.), with the same dimensions and a thickness of around 500 nm. The bulk and thin film samples were irradiated at several fluences with Br

at 25 MeV and Cl at 10 MeV, respectively, in the 5 MV tandetron accelerator at the Centro de Micro-Análisis de Materiales (CMAM) [25]. For Br at 25 MeV (Cl at 10 MeV) the electronic stopping power at the surface is 5.7 keV/nm (3.6 keV/nm) and the projected range is 8.1 μm (4.6 μm); these values were derived from simulations performed using SRIM 2008 [6,26]. The irradiations were performed at room temperature, keeping the current below 10 nA to reduce the heating of the samples.

Two main optical techniques have been used for the characterization of the samples: spectroscopic ellipsometry (SE), and dark-modes (DM) analysis. In the dark-mode method, light of $\lambda = 633$ nm from a He–Ne laser is launched through a glass prism ($n = 1.8315$) into the waveguide generated by irradiation in the silica sample. The incoming incidence angle is varied so that whenever the angle corresponds to a propagating mode the beam is coupled into the waveguide and the reflected beam is lost, appearing as a dark line on the observation screen. In this way one obtains the *effective index* n_m of the mode m, $n_m = n \sin(\theta_m)$, θ_m being the corresponding incidence angle with respect to the normal of the sample. From the effective indices, the refractive index profile at the waveguide is reconstructed from a fit to a solution of the wave equation, using the Wentzel–Kramer–Brillouin (WKB) method [27]. Transverse-electric (TE) and transverse-magnetic (TM) polarization geometries were used to observe any possible differences that might be associated to anisotropy induced during the swift-ion irradiation.

Ellipsometric measurements were carried out at room temperature with an angle of incidence (with respect to the normal of the sample) of 75°, using a spectroscopic ellipsometer of the rotating compensator type (M-2000FI by J.A. Woollam Inc.), in the photon energy range 0.73–5.8 eV. The main ellipsometric equation [28] is $\rho = r_p/r_s = \tan(\Psi)\exp(i \cdot \Delta)$, where ρ is the complex reflectance ratio and r_p and r_s are the Fresnel reflection coefficients for light polarized parallel and perpendicular to the plane of incidence, respectively. Here $\tan(\Psi)$ represents the amplitude ratio upon reflection and Δ the phase shift. SE is a model-based technique where the physical parameters are not directly measured but calculated by minimizing the difference between the measured spectrum of the ellipsometric parameters and the values calculated from the model. The difference was calculated by means of the reduced χ^2 function [29].

3. SE models

The models used in this paper to perform the analysis of the ellipsometric spectra are shown in Fig. 1. In the case of the bulk silica samples, we firstly determined the optical properties (n and k) of virgin silica from a point-by-point direct inversion of the measured $\tan(\Psi)$ and $\cos(\Delta)$ values. Then, the sample with the highest fluence (2×10^{14} cm^{-2}) was analyzed (model shown in Fig. 1a), assuming that the entire irradiated region was completely damaged (i.e., that we have a step-like variation in the refractive index; hence, it was represented using only one layer). From this fit we found the optical properties of the fully-damaged silica and the thickness of the irradiated zone. For the samples with lower fluences we have more complex profiles of refractive indexes; for this reason the damaged region was divided into nine equally spaced effective medium sublayers (this number is rather arbitrary, in this case it was the smallest number of sublayers required to obtain good fits of all the experimental data). All sublayers were composed of a mixture (represented using the effective medium approximation) of virgin and damaged silica (Fig. 1b), obtaining the damaged fraction in each of them from the fit.

In the case of thermal silica, previous to the irradiation we determined the thickness of the SiO_2 thin film and the optical properties of the virgin silica for each sample, using the model

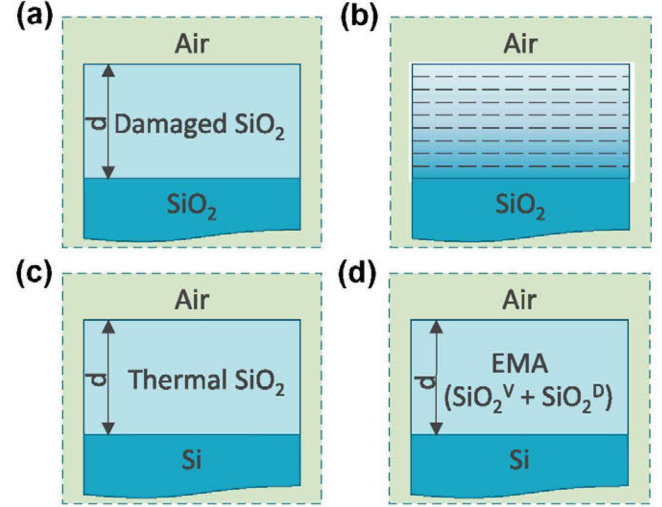

Fig. 1. Schematic representation of the models used to perform the ellipsometric analysis. (a) Only one layer was used to represent the sample with the highest fluence (2×10^{14} cm^{-2}) because it was assumed that the irradiated region was fully damaged. (b) Nine sublayers were necessary for the irradiated region of the samples with lower fluences (1×10^{14} cm^{-2} and below) because they had more complex refractive index profiles. The (c) virgin and (d) damaged thin films were so slim that any in-depth variation of the refractive index was below the sensitivity of the ellipsometer; hence, only one layer was used in both cases.

described in Fig. 1c. It was also assumed in this case that the sample with the highest fluence was totally damaged and then we determined the thickness and refractive index of the fully damaged silica. Finally, the rest of the irradiated samples were analyzed using the effective medium approximation (EMA) to calculate the optical properties of the damaged layer. In particular, this layer was assumed to be composed of a mixture of virgin and compacted (damaged) silica (Fig. 1d).

The Bruggeman model [30] was used to calculate the refractive index of the EMA layers (n_{EMA}) from the optical properties of the constituent elements:

$$f_V \frac{n_V^2 - n_{\mathrm{EMA}}^2}{n_{\mathrm{EMA}}^2 + G(n_V^2 - n_{\mathrm{EMA}}^2)} + f_D \frac{n_D^2 - n_{\mathrm{EMA}}^2}{n_{\mathrm{EMA}}^2 + G(n_D^2 - n_{\mathrm{EMA}}^2)} = 0, \quad (1)$$

where f_V and $f_D = 1 - f_V$ are the virgin and damaged SiO_2 fractions, respectively, n_V (n_D) is the complex refractive index of the virgin (damaged) silica and G is the depolarization factor. In this work we have used a value of 0.5 for G [31,32], corresponding to an isotropic medium with cylindrical inclusions [33]. Moreover, the complex dielectric function ($\varepsilon = \varepsilon_1 + i\ \varepsilon_2$) of the damaged SiO_2 was parameterized by means of cubic splines. The main advantage of this method over analytical representations of the dielectric function is that it favors convergence of the fitting procedures [34].

4. Results

4.1. Spectroscopic ellipsometry of bulk silica samples

Detailed data have been obtained on silica irradiated with Br at 25 MeV whose electronic stopping power at the surface (5.7 keV/nm) is much higher than the nuclear stopping power [35]. In order to analyze the data, we have carried out a first experiment at a high enough fluence to assure that the sample is fully damaged throughout the whole ion range (i.e., that we have obtained a homogeneous damaged layer), Fig. 1a. This is in accordance with a previous study [19] where we found that the irradiated region reaches an uniform steady-state with a well-defined refractive index that is independent on irradiation conditions

(ion type and energy). To test this assumption we left two parameters free for analysis, the refractive index of this final steady-state and the thickness of the layer. The analysis reveals an irradiated layer with a thickness, d, ~7.9 μm that coincides well with the ion range as derived from SRIM simulations (~8.1 μm). The calculated spectral dependence of the real and imaginary part of the refractive index is shown in Fig. 2, together with the spectral dependences assumed for the silica substrate. One observes a clear increase in the extinction coefficient (k) at the visible wavelength range due to the formation of color centers.

For the analysis of the refractive indices at lower irradiation fluences, the top irradiated layer of 7.9 μm was divided into nine sublayers of equal thickness and having a constant refractive index. The results of this step approach are shown in Fig. 3a. From these refractive index profiles one can obtain the damage morphology by using an effective medium approach (see Section 5). For fluences below $4 \times 10^{13}\ cm^{-2}$ there was not enough contrast between the damaged and the virgin regions and, consequently, it was not possible to obtain information of the refractive index profiles.

4.2. Spectroscopic ellipsometry of thermal silica

In this case irradiations were performed with Cl at 10 MeV, having an electronic stopping power of 3.6 keV/nm at the sample surface. One may note that these samples allow taking data at much lower fluences than those analyzed in the previous Section, due to the higher contrast between the silica thin film and the silicon substrate; leading to a more reliable determination of the compaction kinetics. Furthermore, the optical techniques mostly collect information from the initial region, where the nuclear stopping power is almost zero, simplifying the analysis. The calculated film thickness and refractive index before irradiation and after several irradiation fluences are shown in Table 1. One observes that the decrease in thickness (compaction) measured directly reaches a value around 2 %, similar to that inferred in the bulk samples from the index change. Then, the damaged fraction was determined again by means of an effective medium approach. It was assumed that a steady index value was obtained after the highest fluence ($3 \times 10^{13}\ cm^{-2}$).

4.3. Dark-modes

The changes induced by irradiation with Br at 25 MeV in the bulk silica samples were also measured by means of dark modes, in order to facilitate the comparison with the ellipsometric data. The refractive index profiles obtained from the dark modes for various irradiation fluences are shown in Fig. 3b. They show relatively step profiles quite comparable to those obtained from SE and roughly resembling the depth dependence of the electronic stopping power. It is again observed that the index change is saturated somewhat above $10^{14}\ cm^{-2}$.

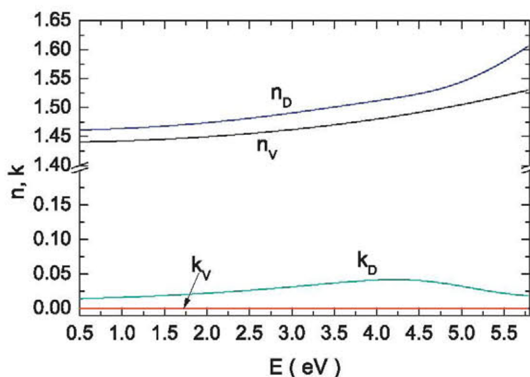

Fig. 2. Real (n) and imaginary (k) part of the refractive index of virgin and damaged silica, obtained from spectroscopic ellipsometry.

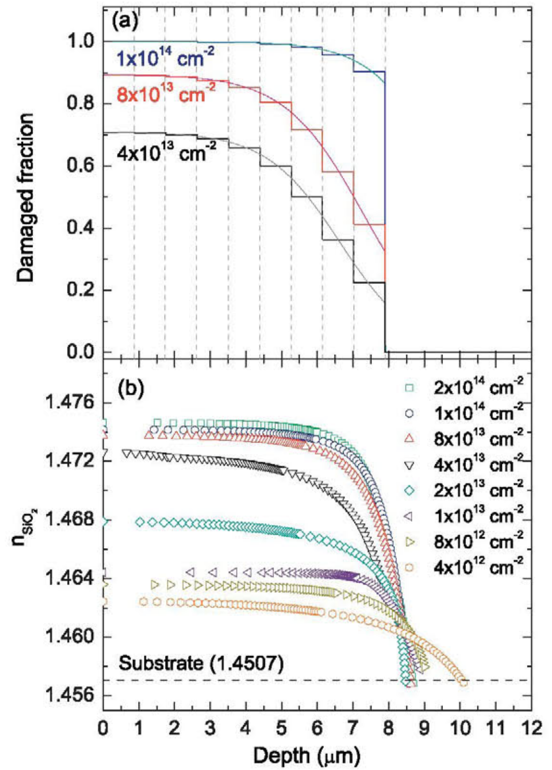

Fig. 3. (a) Damaged fraction and (b) refractive index profiles of bulk silica samples, obtained for various fluences from spectroscopic ellipsometry and dark modes, respectively.

5. Discussion

Both, the ellipsometric and dark-mode data for the refractive index profiles (Fig. 3) are quite consistent and clearly indicate that the changes induced by the irradiation are associated to the electronic stopping power. The compaction effect has been inferred from the change in refractive index for bulk and thermally oxidized samples, assuming proportionality to the crystal density. For the later samples the information has also been directly derived from the change in film thickness brought about by the irradiation. The normalized variation of the dielectric function can be calculated using the expression $\Delta\varepsilon = (\varepsilon_f - \varepsilon_0)/\varepsilon_0$, being ε_0 and ε_f the initial and final dielectric function of silica at the 633 nm wavelength. Likewise, the normalized variation of the thin film thickness is defined by $\Delta d = (d_0 - d_f)/d_0$, being d_0 and d_f the initial and final thickness of the SiO_2 thin films. The data have not shown any evidence of anisotropic deformation of the glassy network. Interestingly, different compaction kinetics and track radii are inferred from the variations of refractive indexes and thicknesses for the thermal silica. To explain this result, it should be recalled that the ion tracks do not have a clearly defined border but instead the damage fraction should fall in a more or less Gaussian way [10] from the center of the track to the undamaged region and, therefore, the radius value obtained by some technique depends on its sensitivity. The described discrepancy suggests that the optical properties are much more sensitive than the thickness to small atomic changes in the silica.

With our optical methods and using an effective medium approach, it has been possible to monitor the evolution of the

Table 1
Ion irradiation parameters for the SiO_2 samples, optical properties as determined from spectroscopic ellipsometry (SE) for both kind of samples and from dark modes (DM) for bulk SiO_2 and thin film thicknesses, determined from SE before (d_0) and after (d_f) the irradiation.

Bulk SiO_2			SiO_2/Si			
Fluence (cm^{-2})	n_{SiO_2} (DM) (633 nm)	n_{SiO_2} (SE) (633 nm)	Fluence (cm^{-2})	n_{SiO_2} (SE) (633 nm)	d_0 (SE) (nm)	d_f (SE) (nm)
Virgin	1.450700	1.4495	Virgin	1.4586	–	–
4.0×10^{12}	1.462435	–	1.0×10^{12}	1.4629	449.3	447.9
8.0×10^{12}	1.463588	–	2.0×10^{12}	1.4651	523.7	519.8
1.0×10^{13}	1.464423	–	4.0×10^{12}	1.4673	500.1	495.5
2.0×10^{13}	1.467885	–	8.0×10^{12}	1.4695	527.0	518.3
4.0×10^{13}	1.472633	1.4662	1.0×10^{13}	1.4702	496.1	486.8
8.0×10^{13}	1.473763	1.4706	2.0×10^{13}	1.4703	519.8	509.5
1.0×10^{14}	1.474178	1.4731	3.0×10^{13}	1.4703	510.2	500.1
4.0×10^{14}	1.474651	1.4731	–	–	–	–

damaged volume of the sample as a function of irradiation fluence. They provide a very useful alternative to the RBS/channeling technique, used to describe the kinetics of amorphization in crystalline materials, and that cannot be applied to amorphous media. SE and DM also present some advantages over IR spectroscopy, which has been mostly used in the past for this task [18,22,23], coming from the possibility of obtaining the depth profile of the refractive index change. Moreover, the IR method relies on a careful decomposition of the absorption spectra into the heavily overlapped bands corresponding to certain ring structures presenting well defined position and width. In this way one obtains structural information that has to be then related to crystal density. Finally, while SAXS have been used to provide estimations of the track radius [16,17] it cannot provide information on the amorphization kinetics and its use is somewhat limited by the required sample preparation. It should be noted that the variations on the refractive index produced by compaction are small (0.02–0.03); however, we have estimated that the experimental error of the methods employed for the determination of the refractive index is $\sim 10^{-3}$ and, consequently, we are able to follow with great accuracy its evolution with the irradiation. Likewise, the error on the measured thin film thicknesses, is also quite small (1–2 nm), due to the high contrast of refractive indices between SiO_2 and Si.

The results derived from ellipsometry and dark-modes are plotted in Fig. 4. Taking into account that such damaged volume is just the accumulation of individual damage tracks one can fit the normalized variation of either the dielectric function or the thin film thickness to a modified Poisson law: $(a[1 - \exp(-\sigma\varphi)]$ [36], which

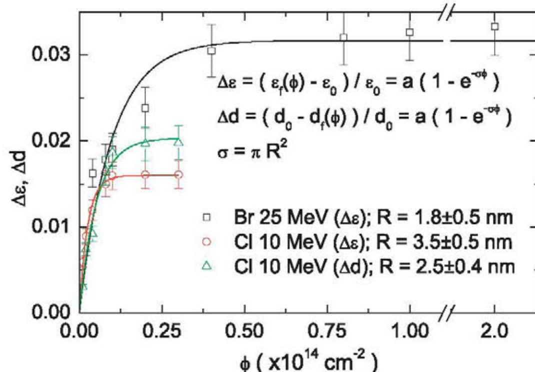

Fig. 4. Normalized variation of either the SiO_2 dielectric function or the thin film thickness. The experimental values were fitted using a modified Poisson law: $a[1 - \exp(-\sigma\varphi)]$, which allowed us to determine first the cross section of the track (σ) and then its radius ($R = \sqrt{\sigma/\pi}$).

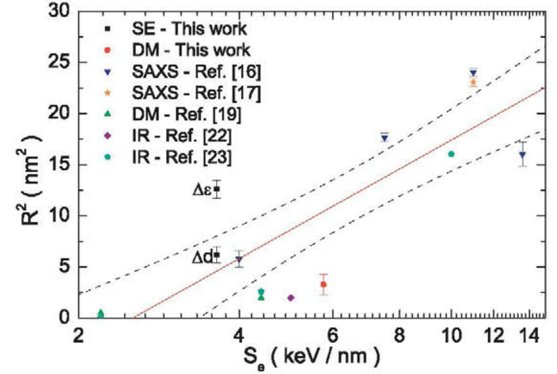

Fig. 5. Track radii in silica as a function of the stopping power at the surface of the sample, obtained from the literature (determined by small-angle X-ray scattering [16,17], dark modes [19] and infrared spectroscopy [22,23]) and from this work (dark modes and spectroscopic ellipsometry). The red continuous line is a fit of the data using the model developed by Szenes [37] and the black dashed lines represent the confidence bands (95%). (For interpretation of the references to color in this figure legend, the reader is referred to the web version of this article.)

allows the determination of the track cross section (σ) and then its radius ($R = \sqrt{\sigma/\pi}$). A track radius of 1.8 ± 0.5 nm was calculated for the bulk silica irradiated with Br at 25 MeV (DM). Similarly, track radii of 2.5 ± 0.4 and 3.5 ± 0.5 nm were found for the SiO_2 thin films irradiated with Cl at 10 MeV from the variations in the film thickness and the refractive index, respectively (SE).

The obtained radii are plotted in Fig. 5, together with data from previous experiments that cover a rather broad range in stopping powers at the surface of the sample. It is remarkable the wide dispersion in the values of the track radii; an effect probably produced by the fact that, as stated above, different techniques "see" different damage thresholds. However, despite the existing dispersion there is a definite trend where below a certain value of stopping power (threshold) there are no tracks. We made a fit of the data using the model developed by Szenes ($R^2 = A \ln (S_e/S_e^t)$; being A a proportionality constant and S_e^t the threshold stopping power) [37], obtaining a value of 2.5 ± 0.4 keV/nm for this threshold, which is very similar to the results obtained by other methods ($\sim$2 keV/nm) [14,21,38,39]. Unfortunately the error of this determination is quite large, making clear that more experimental works would be needed for a more accurate determination of this threshold.

6. Conclusions

In this paper we have determined the damaged fraction induced by swift ion-beam irradiation in silica by spectroscopic ellipsometry and dark-modes. A track radius of 1.8 ± 0.5 nm was calculated from the variations in the refractive index for the bulk silica irradiated with Br at 25 MeV. On the other hand, for the SiO_2 thin films irradiated with Cl at 10 MeV we found track radii of 2.5 ± 0.4 and 3.5 ± 0.5 nm from the variations in the film thickness and the refractive index, respectively. Then, using our values of track radii, together with the data reported in the literature, we were able to estimate a value of $\sim$2.5 ± 0.4 keV/nm for the track formation threshold. Finally, the advantages of the optical methods over some other techniques like RBS/C, IR spectroscopy and small-angle X-ray scattering for the determination of the damaged fraction in amorphous materials have been discussed.

Acknowledgments

We acknowledge financial support from the Spanish Ministry of Science and Innovation for the project MAT-2008-06794-C03-03.

O.P.R. is grateful to Consejo Nacional de Ciencia y Tecnología (CONACyT), Mexico for providing a postdoctoral scholarship.

References

[1] S.I. Najafi, Introduction to Glass Integrated Optics, Artech House Publishers, 1992.
[2] A. Ibarra, E.R. Hodgson, The ITER project: the role of insulators, Nucl. Instrum. Meth. B 218 (2004) 29–35.
[3] C.A. Nicoletta, A.G. Eubanks, Effect of simulated space radiation on selected optical materials, Appl. Opt. 11 (1972) 1365–1370.
[4] D.F. Heath, P.A. Sacher, Effects of a simulated high-energy space environment on the ultraviolet transmittance of optical materials between 1050 A and 3000 A, Appl. Opt. 5 (1966) 937–943.
[5] P.D. Townsend, P.J. Chandler, L. Zhang, Optical Effects of Ion Implantation, Cambridge University Press, 1994.
[6] J.F. Ziegler, The Stopping and Range of Ions in Solids, Pergamon Pr., 1985.
[7] Z.G. Wang, C. Dufour, E. Paumier, M. Toulemonde, The S_e sensitivity of metals under swift-heavy-ion irradiation: a transient thermal process, J. Phys.: Condens. Matter 6 (1994) 6733.
[8] A. Meftah, J.M. Costantini, N. Khalfaoui, S. Boudjadar, J.P. Stoquert, F. Studer, M. Toulemonde, Experimental determination of track cross-section in $Gd_3Ga_5O_{12}$ and comparison to the inelastic thermal spike model applied to several materials, Nucl. Instrum. Meth. B 237 (2005) 563–574.
[9] F. Agulló-López, G. García, J. Olivares, Lattice preamorphization by ion irradiation: fluence dependence of the electronic stopping power threshold for amorphization, J. Appl. Phys. 97 (2005) 093514.
[10] F. Agulló-López, A. Mendez, G. García, J. Olivares, J.M. Cabrera, Synergy between thermal spike and exciton decay mechanisms for ion damage and amorphization by electronic excitation, Phys. Rev. B 74 (2006) 174109.
[11] E. Snoeks, A. Polman, C.A. Volkert, Densification, anisotropic deformation, and plastic flow of SiO_2 during MeV heavy ion irradiation, Appl. Phys. Lett. 65 (1994) 2487–2489.
[12] K. Awazu, S. Ishii, K. Shima, S. Roorda, J.L. Brebner, Structure of latent tracks created by swift heavy-ion bombardment of amorphous SiO_2, Phys. Rev. B 62 (2000) 3689.
[13] N. Khalfaoui, C.C. Rotaru, S. Bouffard, E. Jacquet, H. Lebius, M. Toulemonde, Study of swift heavy ion tracks on crystalline quartz surfaces, Nucl. Instrum. Meth. B 209 (2003) 165–169.
[14] S. Klaumünzer, Ion tracks in quartz and vitreous silica, Nucl. Instrum. Meth. B 225 (2004) 136–153.
[15] T. van Dillen, A. Polman, P.R. Onck, E. van der Giessen, Anisotropic plastic deformation by viscous flow in ion tracks, Phys. Rev. B 71 (2005) 024103.
[16] P. Kluth, C.S. Schnohr, O.H. Pakarinen, F. Djurabekova, D.J. Sprouster, R. Giulian, M.C. Ridgway, A.P. Byrne, C. Trautmann, D.J. Cookson, et al., Fine structure in swift heavy ion tracks in amorphous SiO_2, Phys. Rev. Lett. 101 (2008) 175503.
[17] P. Kluth, C.S. Schnohr, D.J. Sprouster, A.P. Byrne, D.J. Cookson, M.C. Ridgway, Measurement of latent tracks in amorphous SiO_2 using small angle X-ray scattering, Nucl. Instrum. Meth. B 266 (2008) 2994–2997.
[18] M. Toulemonde, W.J. Weber, G. Li, V. Shutthanandan, P. Kluth, T. Yang, Y. Wang, Y. Zhang, Synergy of nuclear and electronic energy losses in ion-irradiation processes: the case of vitreous silicon dioxide, Phys. Rev. B 83 (2011) 054106.
[19] J. Manzano, J. Olivares, F. Agulló-López, M.L. Crespillo, A. Moroño, E. Hodgson, Optical waveguides obtained by swift-ion irradiation on silica (a-SiO_2), Nucl. Instrum. Meth. B 268 (2010) 3147–3150.
[20] L. Skuja, M. Hirano, H. Hosono, K. Kajihara, Defects in oxide glasses, Phys. Stat. Sol. C 2 (2005) 15–24.
[21] M. Toulemonde, S.M.M. Ramos, H. Bernas, C. Clerc, B. Canut, J. Chaumont, C. Trautmann, MeV gold irradiation induced damage in alpha-quartz: competition between nuclear and electronic stopping, Nucl. Instrum. Meth. B 178 (2001) 331–336.
[22] M.C. Busch, A. Slaoui, P. Siffert, E. Dooryhee, M. Toulemonde, Structural and electrical damage induced by high-energy heavy ions in SiO_2/Si structures, J. Appl. Phys. 71 (1992) 2596.
[23] C.C. Stanescu, Ph.D. Thesis, University of Caen/Basse-Normandie, 2002.
[24] A. Rivera, M.L. Crespillo, J. Olivares, G. García, F. Agulló-López, Effect of defect accumulation on ion-beam damage morphology by electronic excitation in lithium niobate: a Monte Carlo approach, Nucl. Instrum. Meth. B 268 (2010) 2249–2256.
[25] CMAM – Centre for Micro Analysis of Materials.<http://www.cmam.uam.es/>, 2011.
[26] J. Ziegler, SRIM – The Stopping and Range of Ions in Matter. <http://www.srim.org/>, 2008.
[27] K.S. Chiang, Construction of refractive-index profiles of planar dielectric waveguides from the distribution of effective indexes, J. Lightwave Technol. 3 (1985) 385–391.
[28] R.M.A. Azzam, N.M. Bashara, Ellipsometry and Polarized Light, North Holland, Amsterdam, 1977.
[29] G.E. Jellison Jr., Data analysis for spectroscopic ellipsometry, Thin Solid Films 234 (1993) 416–422.
[30] D.E. Aspnes, J.B. Theeten, F. Hottier, Investigation of effective-medium models of microscopic surface roughness by spectroscopic ellipsometry, Phys. Rev. B 20 (1979) 3292.
[31] S.-M.F. Nee, Ellipsometric analysis for surface roughness and texture, Appl. Opt. 27 (1988) 2819–2831.
[32] J.E. Spanier, I.P. Herman, Use of hybrid phenomenological and statistical effective-medium theories of dielectric functions to model the infrared reflectance of porous SiC films, Phys. Rev. B 61 (2000) 10437–10450.
[33] Strictly speaking, the tracks are actually more like a cone than like a cylinder, owing to the dependence of the electronic stopping power on the penetration depth. However, considering the huge aspect ratio of the tracks (their height is thousands of times higher than its radius) the assumption of a cylindrical shape does not introduce a considerable error.
[34] M. Garriga, M.I. Alonso, C. Domínguez, Ellipsometry on very thick multilayer structures, Phys. Stat. Sol. B 215 (1999) 247–251.
[35] Additionally, the higher values of the nuclear stopping power are restricted to a narrow zone at the end of the track. In any case, it will have a positive impact, making the border between the irradiated and virgin regions sharper.
[36] A. Meftah, F. Brisard, J.M. Costantini, M. Hage-Ali, J.P. Stoquert, F. Studer, M. Toulemonde, Swift heavy ions in magnetic insulators: a damage-cross-section velocity effect, Phys. Rev. B 48 (1993) 920–925.
[37] G. Szenes, General features of latent track formation in magnetic insulators irradiated with swift heavy ions, Phys. Rev. B 51 (1995) 8026–8029.
[38] A. Meftah, F. Brisard, J.M. Costantini, E. Dooryhee, M. Hage-Ali, M. Hervieu, J.P. Stoquert, F. Studer, M. Toulemonde, Track formation in SiO_2 quartz and the thermal-spike mechanism, Phys. Rev. B 49 (1994) 12457–12463.
[39] J. Manzano-Santamaría, J. Olivares, A. Rivera, F. Agulló-López, Electronic damage in quartz (c-SiO_2) by MeV ion irradiations: potentiality for optical waveguiding applications, Nucl. Instrum. Meth. B 272 (2012) 271–274.